THE PHOTOSPHERIC BARIUM SPECTRUM: SOLAR ABUNDANCE AND COLLISION BROADENING OF Ba II LINES BY HYDROGEN

HARTMUT HOLWEGER

Institut für Theoretische Physik und Sternwarte der Universität Kiel, Kiel, F.R.G.

and

EDITH A. MÜLLER

Observatoire de Genève, Sauverny, Switzerland

(Received 15 May, 1974)

Abstract. A study of the solar Ba II spectrum leads to a *solar abundance of barium* of $\log \varepsilon_{\mathrm{Ba}} = 2.11 \pm 0.12$, on the scale $\log \varepsilon_{\mathrm{H}} = 12$. The observed asymmetry of the resonance line $\lambda 4554$ is consistent with an *isotopic abundance ratio* equal to the terrestrial one. The *meteoritic* Ba/Si abundance ratio found in carbonaceous chondrites appears to exceed the solar ratio by 0.1 to 0.2 dex (Section 5).

The *broadening by collisions with hydrogen atoms* is determined from the solar spectrum (Section 4). Damping half-widths, γ_{H}, of the three stronger Ba II lines turn out to be larger by a factor of about 3.0 than predicted from pure van der Waals interaction of dipoles.

Departures from LTE appear to be present in the cores of the resonance lines and of the lines arising from the metastable $5D$ levels (Section 6). The equivalent widths, however, remain practically unaffected.

Equivalent widths of *neutral barium* lines are predicted and some new identifications of photospheric Ba I lines are suggested (Section 7).

1. Introduction

Barium, though represented in stellar spectra by only a few lines, plays an important role in stellar spectroscopy as one of the key elements to nucleosynthesis. In the solar spectrum, barium appears predominantly in its first ionization state. Generally, the Ba II lines are not weak. Thus, in abundance determination, uncertainties arise from the fact that thermal broadening of this heavy element is small and, therefore, other broadening mechanisms like hyperfine structure, microturbulence, and damping are becoming important. In the present work we study influence and magnitude of these parameters, using model atmosphere techniques and assuming local thermodynamic equilibrium.

2. Solar and Atomic Data of Ba II

The Fraunhofer lines suitable for abundance determination are listed in Table I. The equivalent widths of the three relatively strong unblended lines (multiplets 1 and 2) were measured on high dispersion spectrograms secured with the McMath solar spectrograph of the Kitt Peak National Observatory. The profiles of the remaining three lines were taken from Jungfraujoch tracings (Delbouille *et al.*, 1973). These weaker lines require special care because they are more or less severely blended and, in addition,

Solar Physics **39** (1974) 19–30.

TABLE I

Ba II lines: solar and atomic data

$\Delta r^2/a_0^2$ = mean square radius (upper minus lower level) used for calculating damping constants. Equivalent widths W_λ refer to center of disk. $\Delta \log \varepsilon$ = abundance change corresponding to the empirical adjustment of pure van der Waals damping (Section 4); the resulting abundances are given in the last row

	Mult. No.	$\lambda_\odot$ (Å)	Transition	Lower E.P. (eV)	$\Delta r^2/a_0^2$	log gf	W_λ (mÅ)	$\Delta \log \varepsilon$	$\log \varepsilon$
Ba II	1	4554.036	$6S_{1/2}$–$6P_{3/2}$	0.00	12	+0.17	189	−0.36	2.06
	2	6496.908	$5D_{3/2}$–$6P_{1/2}$	0.60	20	−0.38	101	−0.26	2.13
		5853.688	$5D_{3/2}$–$6P_{3/2}$	0.60	22	−1.00	62	−0.12	2.13
	3	4524.944	$6P_{1/2}$–$7S_{1/2}$	2.50	55	−0.54	30 [a]	−0.03	2.88
	4	4130.657	$6P_{3/2}$–$6D_{5/2}$	2.71	44	+0.56	33 [a]	−0.03	2.06
		3891.781	$6P_{1/2}$–$6D_{3/2}$	2.50	44	+0.23	31 [a]	−0.03	2.17

[a] Note: *calculated* W_λ, using the abundance determined by spectrum synthesis and assuming an unperturbed continuum. The λ4524 line has been excluded from the final results (see Section 4).

the location of the continuum is uncertain. Instead of measuring their equivalent widths, we used the method of spectrum synthesis, calculating the whole spectral region around each line by adjusting the abundance properly to obtain a best fit. In the case of λ3891, the Balmer line H_8 (λ3889.1) was also included in the blend calculation.

To check for the influence of a quasi-continuum produced by numerous overlapping weak lines, we made test calculations without changing the abundance but including an additional opacity of 10% of the continuous opacity, simulated by Fe I lines of an average excitation potential of 3 eV. No noticeable deterioration of the profile fit occurred, that is, the intensities relative to the local quasi-continuum remained unchanged.

The uncertainty of the barium abundance introduced by blending and by depression of the true continuum is estimated to be less than 0.05 dex for the three weaker lines in question.

The *oscillator strenghts* given in Table I are from Hanle-effect measurements by Gallagher (1967) for multiplets 1 and 2, and from quantum-mechanical calculations (scaled Thomas-Fermi method) by Warner (1968) for multiplets 3 and 4. Since Ba II is a one-electron system, theoretical f-values should be quite reliable. Indeed, they agree closely with Gallagher's measurements in the case of multiplets 1 and 2.

Radiative damping was included in our computations by appropriately summing, for each level, the transition probabilities tabulated by Miles and Wiese (1969). Neglecting radiative damping would lead to a 0.10 dex too high an abundance inferred from the resonance line, the other lines being less sensitive.

Broadening by electron collisions was calculated using the measurements by Jäger (1969). This kind of broadening is even less effective than radiative damping; omitting it increases the abundance by at most 0.03 dex (λ4554 Å).

Broadening by neutral perturbers (hydrogen) was first calculated by assuming pure van der Waals interaction and calculating the interaction constants from the dipole approximation given by Unsöld (1955, Equation 82, 54). In Section 4 we determine empirically the deviations from this interaction by proceeding along the same line as Holweger (1972) comparing weak and strong lines.

Hyperfine structure has also been taken into account. The main isotopes are Ba 135 (7%), Ba 136 (8%), Ba 137 (11%), and Ba 138 (72%). The percentage values given in parentheses correspond to the terrestrial isotopic ratios. We adopted these ratios in the computation of the solar line profiles (for further dicussion see Section 5). HFS data for various barium lines and the corresponding levels were published by Ritschl and Sawyer (1931), Murakawa (1932), and by Brix and Kopfermann (1952). The isotopic shift is negligible compared to the splitting due to the nuclear moment associated with the odd isotopes. The lines of multiplet 2 are not included in the measurements cited. The splitting of their lower level $5D_{3/2}$ is unknown but probably much smaller than that of the upper term $6P$ with its deep-penetrating electron orbit. Indeed, the next higher term, $6D$, has been found single (Murakawa, 1932). Thus we have assumed that the HFS of multiplet 2 is due only to the known splitting of the $6P$ term, which itself is about $\frac{1}{6}$ of the ground state splitting. The effect of HFS on abundances turned out to be significant only for the resonance line, λ4554. Neglecting HFS would result in a 0.12 dex too high an abundance inferred from the equivalent width of this line. For λ6496 and λ5853 the figures are 0.03 and 0.02 dex, respectively. The profiles of the remaining three weak lines are practically unaffected, their central intensities change by less than 0.5% of the continuum intensity.

3. Solar Model Atmosphere

The solar model atmosphere used is given in Table II. Gas and electron pressure were calculated assuming the following abundances ($\log\varepsilon$) of the electron contributing elements, H: 12, He: 11.00, Mg: 7.60, Si: 7.65, Fe: 7.60. Because the nature of small-scale hydrodynamic phenomena in the solar atmosphere is not well understood we prefer to treat their combined effect on line profiles schematically in terms of microturbulence. In addition, a depth-independent macroturbulence $V = 1.6\ \mathrm{km\ s^{-1}}$ as determined provisionally by Garz *et al.* (1969) was included in the hydrostatic equilibrium and used also for the line-profile calculations, assuming a Gaussian distribution $\exp(-v^2/V^2)$. The value of $1.0\ \mathrm{km\ s^{-1}}$ of the microturbulence near $\tau_{5000} = 0.1$ seems rather well established from equivalent widths of different elements (see, e.g. May *et al.*, 1974). Its depth-dependence is still uncertain, though most recent investigators agree in a decrease with height (Lites, 1973). A depth-independent microturbulence of $1.0\ \mathrm{km\ s^{-1}}$ would have no serious effect on the abundance. It would result in a decrease by 0.01 dex in the final abundances of the three stronger lines, and an increase by 0.04 dex for the weaker lines. Contrary to this insensitivity, an overall reduction of the microturbulence by $0.2\ \mathrm{km\ s^{-1}}$ leads to a noticeable increase of the abundance as follows, for λ4554: +0.03, for $\lambda\lambda$6496 and 5853: +0.12, for the other lines: +0.04 dex.

TABLE II

Solar model atmosphere used in the present work. The model of Holweger (1967) has been updated with respect to chemical composition and continuum intensity. The microturbulence ξ (vertical component) has also been changed in accordance with Garz *et al.* (1969)

$\bar{\tau}_R$	$\log \bar{\tau}_R$	$\log \tau_{5000}$	T	$\log P_g$	$\log P_e$	ξ
2.0E-7	−6.699	−6.539	3900	+0.769	−3.140	
2.5E-7	−6.602	−6.279	3920	+1.171	−2.752	
5.0E-7	−6.301	−5.868	3970	+1.598	−2.342	
1.0E-6	−6.000	−5.588	4030	+1.842	−2.105	
2.0E-6	−5.699	−5.334	4080	+2.042	−1.910	
5.0E-6	−5.301	−5.001	4160	+2.279	−1.674	
1.0E-5	−5.000	−4.747	4210	+2.450	−1.508	
2.0E-5	−4.699	−4.486	4270	+2.618	−1.341	
5.0E-5	−4.301	−4.131	4340	+2.835	−1.128	
1.0E-4	−4.000	−3.856	4400	+2.999	−0.967	0.50
2.0E-4	−3.699	−3.577	4460	+3.162	−0.804	0.50
5.0E-4	−3.301	−3.200	4530	+3.377	−0.596	0.50
0.001	−3.000	−2.912	4590	+3.541	−0.437	0.50
0.002	−2.699	−2.621	4640	+3.704	−0.279	0.50
0.005	−2.301	−2.233	4720	+3.919	−0.070	0.50
0.01	−2.000	−1.939	4800	+4.083	+0.094	0.50
0.02	−1.699	−1.645	4900	+4.245	+0.266	0.65
0.05	−1.301	−1.256	5080	+4.460	+0.504	0.85
0.10	−1.000	−0.961	5260	+4.622	+0.705	1.00
0.25	−0.602	−0.571	5560	+4.830	+1.002	1.25
0.40	−0.398	−0.371	5850	+4.926	+1.251	1.40
0.70	−0.155	−0.133	6260	+5.022	+1.613	1.50
1.0	0.000	+0.019	6570	+5.070	+1.879	1.60
1.5	+0.176	+0.191	6880	+5.114	+2.140	1.70
2.0	+0.301	+0.312	7160	+5.140	+2.363	1.80
4.0	+0.602	+0.597	7920	+5.191	+2.889	1.80
6.0	+0.778	+0.761	8250	+5.213	+3.092	1.80
8.0	+0.903	+0.877	8420	+5.229	+3.196	1.80
10	+1.000	+0.967	8500	+5.242	+3.245	1.80

The *temperature* model of Table II differs in the deep photosphere ($\tau_{5000} > 0.1$) by 40 K from Holweger's model (1967). This minor correction was necessary to compensate for the change of atmospheric structure due to the altered chemical composition. It ensures agreement of continuum intensity with the measurements performed and compiled by Labs and Neckel (1968; 1970; 1972) and Gingerich *et al.* (1971), covering the visible and infrared spectral region (5000 Å to 300 μ).

In addition to this model we used the HSRA (Gingerich *et al.*, 1971) for comparison. The HSRA yields somewhat lower abundances. The abundance changes are as follows, λ4554: −0.06, $\lambda\lambda$6496 and 5853: −0.10, other lines: −0.04. The inner damping wings of strong Fraunhofer lines, such as Mg I λ5173, are less well reprocuded by the HSRA. According to Gingerich *et al.* it is comparatively poorly determined around $\tau_{5000} = 0.01$.

The elaborate theoretical solar model recently published by Kurucz (1974) has a temperature profile which is remarkably similar to that of our model.

4. Broadening of Ba II Lines by Hydrogen: Results

When calculating the broadening by hydrogen with the van der Waals approximation, the abundances resulting from different lines (disregarding for a moment the $\lambda 4524$ line) show a general apparent increase with equivalent width. We interpret this as an inadequate representation of the interatomic potential. Clearly, the van der Waals formula used is of approximative character, implying, for example, dipole-dipole interaction. Furthermore, as Roueff and Van Regemorter (1969) first pointed out, repulsive forces due to close encounters are probably a much more efficient broadening mechanism.

We may determine the broadening by hydrogen of the three stronger lines by properly adjusting it to make their abundances agree with the abundance obtained from the weak lines. Reasonable agreement is achieved by formally increasing the van der Waals interaction constant C_6 by $\Delta \log C_6 = +1.2 \pm 0.4$. This corresponds to an *enhancement of the damping half width* γ_H *by a factor of about 3.0 over the van der Waals value.* The rather large uncertainties due to the small number of lines would admit factors ranging from 2.0 to 4.0. The resulting abundances are listed in the last column of Table I and shown in Figure 1. In the second to last column of the same table we give the differences in the abundances ($\Delta \log \varepsilon$) derived with the van der Waals approximation and with the empirical adjustment of the broadening by hydrogen.

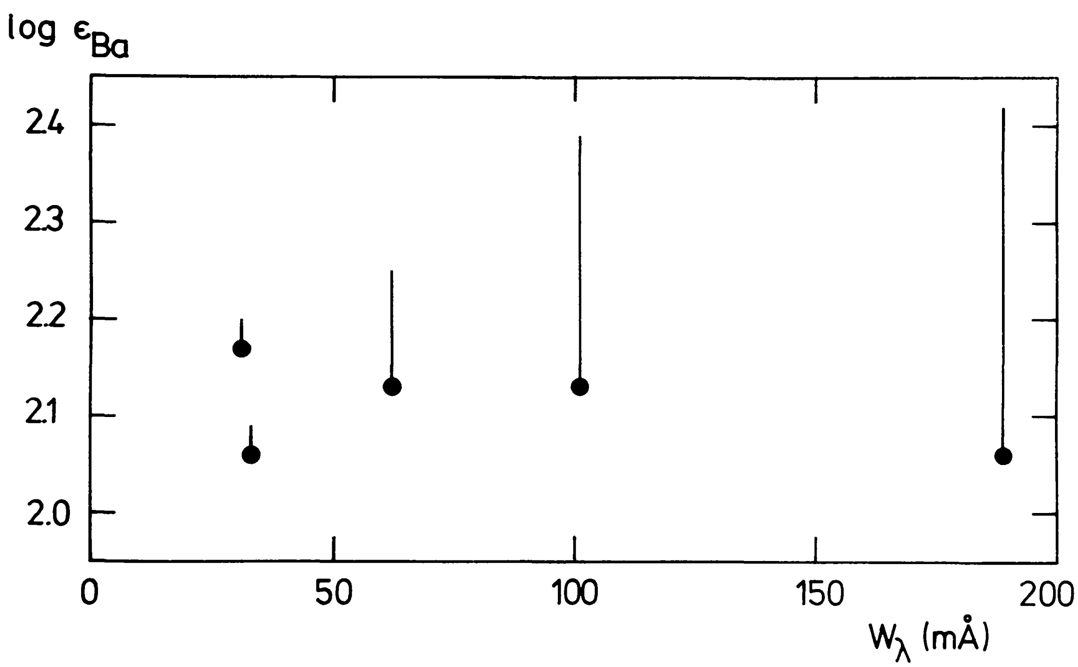

Fig. 1. Barium abundances computed from individual Ba II lines. Dots: broadening by hydrogen increased by a factor of 3.0 over pure van der Waals broadening determined with Unsöld's approximation. Vertical bars indicate how the situation changes if no such empirical correction is applied.

Similar factors were found by the same method for Ca I (3.0), Ca II (1.7), and Na I (2.1) (Holweger, 1972). For the sodium D lines independent theoretical investigations yielded an enhancement factor of 1.5 (Lewis *et al.*, 1971) and 2.2 (Roueff, 1972). This may be considered as a verification of the 'solar absorption tube' results, which are, however, applicable only to stellar atmospheres and not to – usually much denser – laboratory plasmas. A theoretical explanation of the similarity of these enhancement factors is beyond the scope of the present work. We might mention Brueckner's (1971) theoretical results for various Fe I transitions, yielding similarly uniform factors in the range 2.0 to 3.6.

The λ4524 line requires special discussion because it leads to an exceedingly high abundance, i.e., $\log \varepsilon = 2.88$. This peculiarity was also noted by Lambert and Warner (1968). No broadening mechanisms can account for this discrepancy of a factor of 6. That the f-value of this particular transition ($6P$–$7S$) is in error by such a large factor seems unlikely but cannot be excluded unless accurate measurements are available. An alternative explanation is that an unknown line of another element dominates the barium line. We have made efforts to identify the perturber which seems to be responsible also for the rather broad wings not reproduceable by a barium line. We consulted the tables of Moore (1959), Kiess *et al.* (1961) and Banks *et al.* (1967), without success. The MIT tables (Harrison, 1939) indicate that the wings of λ4524.944 may be affected by Co I λ4524.933 and by Os I λ4524.869. We estimated the equivalent widths of these lines, using other isolated lines of the same element together with their laboratory intensities. Both lines seem to be as weak as 2 to 4 mÅ. A search for faint Fe I lines, kindly performed by Mrs T. Garz at the Institut für Experimentalphysik in Kiel, yielded no line of a solar equivalent width exceeding 5 mÅ. Furthermore we examined the chromospheric identification lists of Dunn *et al.* (1968) and Pierce (1968) but could not find indications for possible blending lines. If the perturber were a low-excited neutral atom, the line should be greatly enhanced in the spectrum of Arcturus (R. Mäckle, private communication). The Arcturus atlas (Griffin, 1968) shows the line but not clearly enhanced. In sunspot spectra the line appears to be weaker as compared to the photospheric spectrum (Moore *et al.*, 1966). The question remains open, and we follow Lambert and Warner and omit this line from further discussion.

5. Solar and Meteoritic Barium Abundance. Isotopic Ratio

The mean *solar barium abundance* we obtain from Figure 1 and Table I (excluding the result from λ4524) is

$$\log \varepsilon_{\mathrm{Ba}} = 2.11 \pm 0.12$$

on the scale of $\log \varepsilon_{\mathrm{H}} = 12$. The error limits given represent an overall estimate and are due primarily to the small number of usable lines, only two of them being relatively weak.

Previous abundance determinations from Ba II lines lead to $\log \varepsilon_{\mathrm{Ba}} = 2.10$ (Goldberg *et al.*, 1960) and $\log \varepsilon_{\mathrm{Ba}} = 1.90$ (Lambert and Warner, 1968). Both analyses differ from the present one with respect to the observational data, the assumed model, microturbulence (both used 1.8 km s^{-1}) and damping.

The *meteoritic abundance* obtained from carbonaceous chondrites of type 1 is Ba/Si$=4.7\times10^{-6}$ by number, according to the compilation by Urey (1967). This abundance is based on the analysis of the Orgueil meteorite by Reed *et al.* (1960). The same authors also analysed other types of meteorites which show higher dregree of metamorphism and fractionation. Since their results are given in ppm, we have converted then into abundances (by number) relative to Si, using the corresponding Si concentrations tabulated by Moore (1971). The figure quoted by Urrey served as a check for this conversion. In order to compare with the solar abundance we normalised the meteoritic silicon abundance in accordance with the solar abundance obtained from recently measured *f*-values (Garz, 1973; Holweger, 1973), $\log\varepsilon_{Si}=7.65\pm0.07$. The resulting meteoritic barium abundances ($\log\varepsilon_{Ba}$) are as follows:

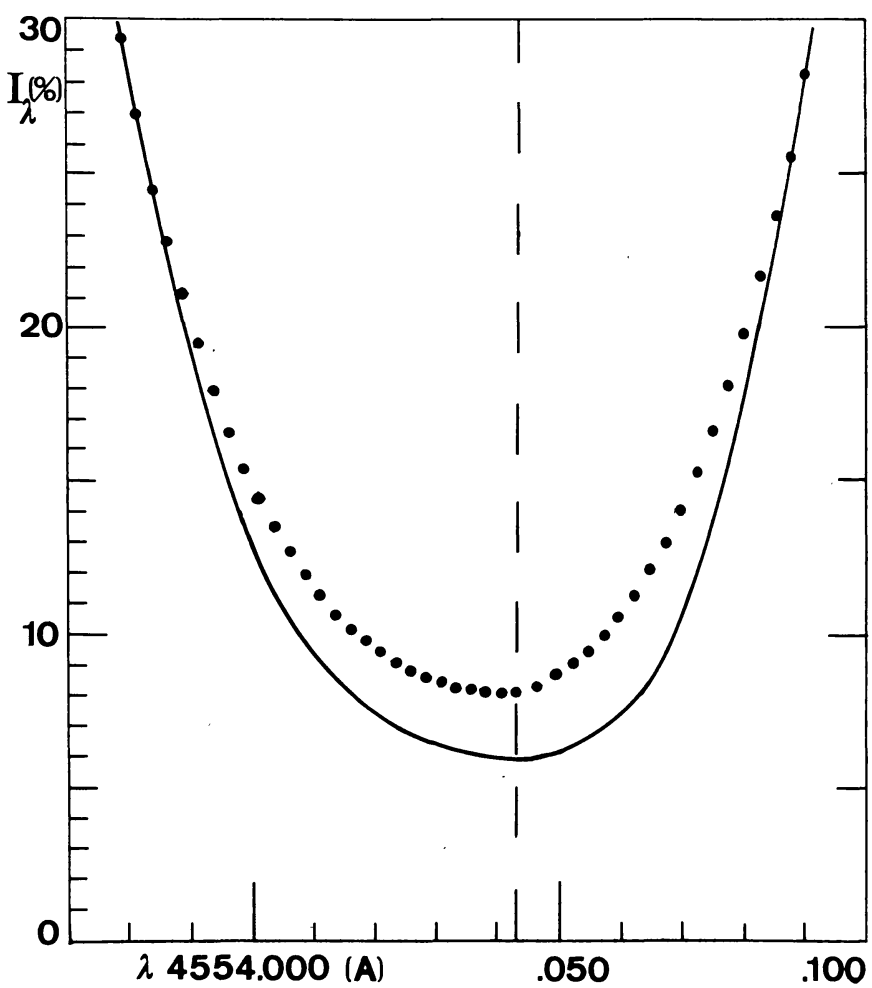

Fig. 2. Core of the Ba II resonance line λ4554.04, showing asymmetry due to the various barium isotopes. Full line: observed profile. Dots: computed profile (LTE) assuming terrestrial isotopic abundance ratio. The vertical line marks the deepest point of the profile. The solar profile is from Delbouille *et al.* (1973), and is not corrected for the (small) effect of the finite resolving power of the spectrograph.

Carbonaceous chondrites C1 (Orgueil)	2.32
Carbonaceous chondrites C2 (Mighei)	2.24
Ordinary chondrites	2.23
Enstatite chondrites	1.97.

Comparing these values with the solar result, 2.11 ± 0.12, *it appears that the* Ba/Si *abundance ratio is slightly different in the Sun and in* C1 *chondrites*. Whether this is significant and possibly due to some fractionation process in the early solar nebula of the kind discussed by Anders (1971), cannot be decided from the rather meager solar barium spectrum.

The profile of the Ba II resonance line $\lambda 4554$ offers a simple way of estimating the *solar isotopic ratio*, because this line has a rather wide hyperfine structure due to the S term involved. As stated in Section 2, our line profile computations were carried out using the *terrestrial* isotopic abundance ratio, the isotopes Ba 135, 136, and 137 contributing a total of 26%. The main isotope, Ba 138 (72%), has zero nuclear moment. The computed line profile shows a clear asymmetry in the core, caused by the contribution of the less abundant isotopes. This same asymmetry is found in the solar line profile of both the Kitt Peak and the Jungfraujoch spectrograms. Figure 2 shows a nearly perfect agreement of shape of the line core, apart from a vertical displacement which will be discussed below. We conclude that the ratio of the less abundant barium isotopes to Ba 138 is essentially *the same in the Sun and in terrestrial matter.*

6. Line Cores: Departures from LTE in High Atmospheric Layers

In an earlier study of central intensities of Fraunhofer lines Holweger (1967) found that the cores of the three stronger Ba II lines were not satisfactorily reproduced by the solar model, in contrast to the great majority of other lines. Hyperfine structure and non-LTE effects were thought responsible for this. The better observational material available now leads to a more detailed picture.

As shown in Figure 2, the observed core of the resonance line $\lambda 4554$ is about 2% deeper than predicted by our LTE calculations (model of Section 3, macroturbulence $V = 1.6$ km s^{-1}, $\Delta \log C_6 = +1.2$, terrestrial isotopic abundance ratio).

Much larger deviations in the same direction are present for the lines of multiplet 2, $\lambda\lambda 6496$ and 5853, the difference amounting to 12% and 8%, respectively, of the continuum intensity. In all three cases these departures are restricted to the line cores, $\Delta\lambda \approx \pm 25$ to ± 35 mÅ, depending on line strength. The remaining part of the profile, originating in optical depths $\tau_{5000} \gtrsim 0.01$, is satisfactorily reproduced. The equivalent width is affected by only about 4 mÅ in the worst case, i.e., $\lambda 6496$, and by less than 2 mÅ in the other cases. Figure 3 illustrates the $\lambda 6496$ line profile observed at Kitt Peak (full line) and the predicted profiles resulting from our LTE calculations. The open circles represent the results without macroturbulence, the dots show the theoretical profile convoluted with a Gaussian distribution corresponding to a macroturbulence $V = 1.6$ km s^{-1}.

It is interesting to note that just those lines which show the largest deviations originate

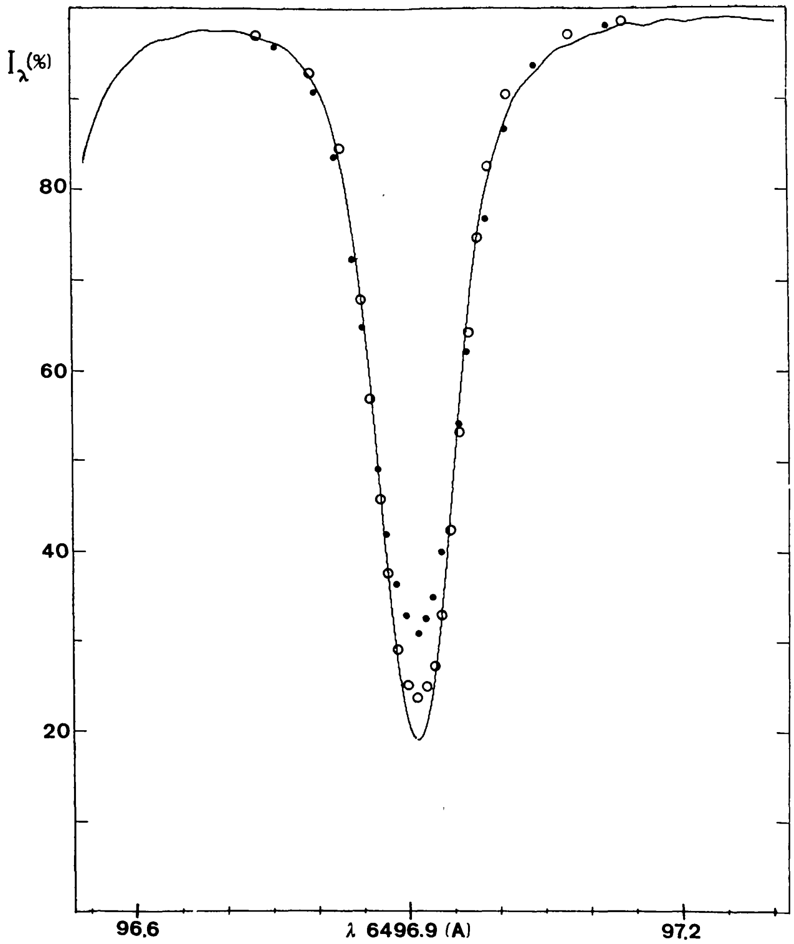

Fig. 3. Solar line profile of Ba II λ6496.91 (full line) observed at KittPeak National Observatory. As in Figure 2, the theoretical profiles were calculated with the model of Section 3 and $\Delta \log C_6 = +1.2$. Open circles: no macroturbulence; dots: with macroturbulence $V = 1.6$ km s^{-1}.

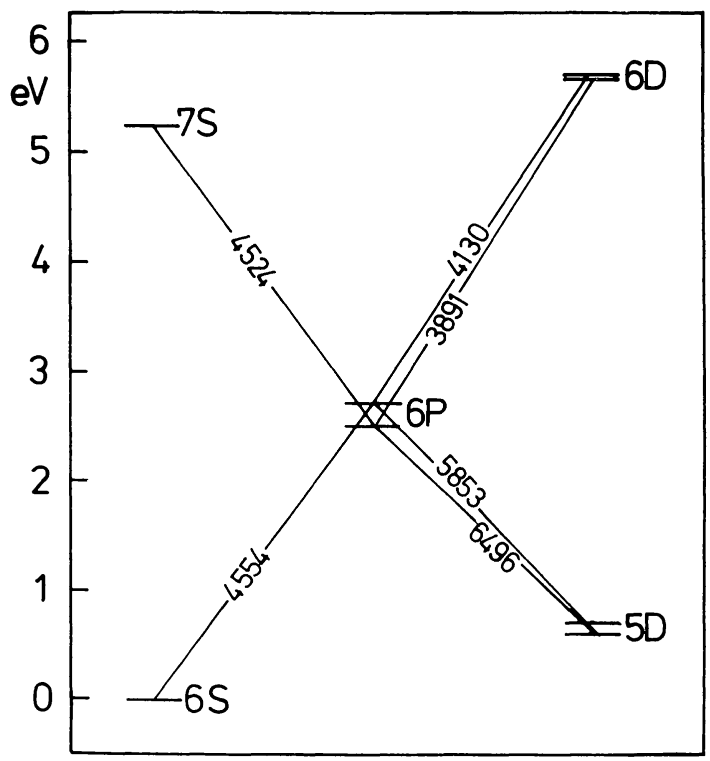

Fig. 4. Term diagram of Ba II showing the transitions studied in this work.

from the metastable $5D$ term (Figure 4). This supports the view that the cores of the stronger Ba II lines are affected by departures from LTE occurring in high atmospheric layers, i.e., $\tau_{5000} < 0.01$. We may point out that this result demonstrates the usefulness of the LTE technique, being able to detect a beginning failure of the physical asssumptions involved.

7. Solar Ba I Lines: Predicted Equivalent Widths and New Identifications

The Revised Rowland Table (Moore *et al.*, 1966) lists only 2 photospheric lines of neutral barium. One of them, λ5535.5, is heavily perturbed; its existence can only be inferred from the sunspot spectrum where the line appears greatly strengthened. The other line, λ6498.8, is quoted as questionable.

It may be useful to know the equivalent widths that are to be expected for the strongest and least perturbed Ba I lines. Table III presents the results of a straightforward calculation, using the barium abundance obtained in Section 5 and the oscillator strengths tabulated by Miles and Wiese (1969).

TABLE II

Predicted equivalent widths of selected Ba I *lines* (center of solar disk). Wavelengths are from Moore (1959)

	Mult. No.	λ(Å)	Lower E.P. (eV)	$\log gf$	w_λ(mÅ)	Solar identification
Ba I	1	7911.338	0.00	−2.00	0.02	–
	2	5535.484	0.00	+0.20	3.5	masked
	6	6498.759	1.18	+0.58	0.8	confirmed
		6527.312	1.14	+0.27	0.4	masked
	7	6110.784	1.18	+0.44	0.5	new
		6063.117	1.14	+0.21	0.3	new
	9	5777.622	1.67	+0.72	0.3	new
	10	7905.751	1.67	+0.25	0.1	–

We have checked for possible identifications by looking through the Jungfraujoch and Kitt Peak solar spectrum atlases (Delbouille and Roland, 1963; Delbouille *et al.*, 1973; Brault and Testerman, 1972). The $\lambda\lambda$7911 and 7905 lines are too weak to be detectable. The strongest line, λ5535, is completely masked by two adjacent strong lines; λ6498 is present and has an equivalent width of about 0.5 mÅ, in reasonable agreement with the prediction of Table III. Thus the tentative identification by Moore *et al.* is confirmed. The line at λ6527.312 is hardly visible because of Si I λ6527.215. Two clear new identifications are $\lambda\lambda$6110 and 6063; we measured their equivalent widths on the extended-scale tracings of the Jungfraujoch atlas and found $W_\lambda \approx 0.3$ mÅ. These lines are listed but not identified in the Rowland table. A further new identification is probably λ5777, a weak feature of 0.1 to 0.2 mÅ equivalent width.

We may conclude that the observed Ba I lines are consistent with the barium abundance derived in Section 5.

Acknowledgements

We are grateful to L. Delbouille and G. Roland for providing Jungfraujoch records prior to publication. E. A. M. expresses her sincere gratitude to the director and the entire staff of the Kitt Peak National Observatory, in particular to A. K. Pierce, J. W. Brault, and L. Testerman, for the allocation of observing time, their warm hospitality and their kind cooperation during her stay in Tucson. H. H. wishes to thank the staff members of the Geneva Observatory for their kind hospitality. Computations were carried out at the Centre Cantonal Informatique de l'Université de Genève and at the Rechenzentrum der Universität Kiel. This work was supported in part by the Fonds National Suisse de la Recherche Scientifique.

References

Anders, E.: 1971, *Ann. Rev. Astron. Astrophys.* **9**, 1.

Banks, H. W., Bozman, W. R., and Wilson, Ch. M.: 1967, Georgetown Obs. Monograph No. 20.

Brault, J. and Testerman, L.: 1972, Preliminary Edition of the Kitt Peak Solar Atlas, Kitt Peak National Observatory, Tucson, Arizona.

Brix, P. and Kopfermann, H.: 1952, *Landolt-Börnstein I/5*, Springer, Berlin-Göttingen-Heidelberg.

Brueckner, K. A.: 1971, *Astrophys. J.* **169**, 621.

Delbouille, L. and Roland, G.: 1963, *Atlas photométrique du spectre solaire de* λ7498 *à* λ12016, Institut d'Astrophysique de l'Université de Liège, Liège.

Delbouille, L., Roland, G., and Neven, L.: 1973, *Atlas photométrique du spectre solaire de* λ3000 *à* λ10000, Institut d'Astrophysique de l'Université de Liège, Cointe-Ougrée.

Dunn, R. B., Evans, J. W., Jefferies, J. T., Orrall, F. Q., White, O. R., and Zirker, J. B.: 1968, *Astrophys. J. Suppl.* **15**, 275.

Gallagher, A.: 1967, *Phys. Rev.* **157**, 24.

Garz, T.: 1973, *Astron. Astrophys.* **26**, 471.

Garz, T., Holweger, H., Kock, M., and Richter, J.: 1969, *Astron. Astrophys.* **2**, 446.

Gingerich, O., Noyes, R. W., Kalkofen, W., and Cuny, Y.: 1971, *Solar Phys.* **18**, 347.

Goldberg, L., Müller, E. A., and Aller, L. H.: 1960, *Astrophys. J. Suppl.* **5**, 1.

Griffin, R. F.: 1968, *A Photometric Atlas of the Spectrum of Arcturus*, Cambridge Philosophical Society, Cambridge.

Harrison, G. R.: 1939, *Wavelength Tables*, Mass. Inst. Technology, Wiley, New York.

Holweger, H.: 1967, *Z. Astrophys.* **65**, 365.

Holweger, H.: 1972, *Solar Phys.* **25**, 14.

Holweger, H.: 1973, *Astron. Astrophys.* **26**, 275.

Jäger, H.: 1969, *Z. Physik* **223**, 19.

Kiess, C. C., Rubin, V. C., and Moore, Ch. E.: 1961, *J. Res. Nat. Bur. Stand.* **65A**, 1.

Kurucz, R. L.: 1974, *Solar Phys.* **34**, 17.

Labs, D. and Neckel, H.: 1968, *Z. Astrophys.* **69**, 1.

Labs, D. and Neckel, H.: 1970, *Solar Phys.* **15**, 79.

Labs, D. and Neckel, H.: 1972, *Solar Phys.* **22**, 64.

Lambert, D. L. and Warner, B.: 1968, *Monthly Notices Roy. Astron. Soc.* **140**, 197.

Lewis, E. L., McNamara, L. F., and Michels, H. H.: 1971, *Phys. Rev.* **A3**, 1939.

Lites, B.: 1973, *Solar Phys.* **32**, 283.

May, M., Richter, J., and Wichelmann, J.: 1974, *Astron. Astrophys.*, to be published.

Miles, B. M. and Wiese, W. L.: 1969, Nat. Bur. Stand. Technical Note 474.

Moore, C. B.: 1971, in B. Mason (ed.), *Handbook of Elemental Abundances in Meteorites*, Gordon and Breach, New York, p. 125.

Moore, Ch. E.: 1959, Nat. Bur. Stand. Technical Note 36.

Moore, Ch. E., Minnaert, M. G. J., and Houtgast, J.: 1966, Nat. Bur. Stand. Monograph 61.

Murakawa, K.: 1932, *Sci. Pap. Inst. Phys. Chem. Res. Tokyo* **18**, 304.

Pierce, A. K.: 1968, *Astrophys. J. Suppl.* **17**, 1.
Reed, G. W., Kigoshi, K., and Turkevich, A.: 1960, *Geochim. Cosmochim. Acta* **20**, 122.
Ritschl, R. and Sawyer, R. A.: 1931, *Z. Physik* **72**, 36.
Roueff, E.: 1972, *Phys. Letters* **38A**, 8.
Roueff, E. and Van Regemorter, H.: 1969, *Astron. Astrophys.* **1**, 69.
Unsöld, A.: 1955, *Physik der Sternatmosphären*, Springer, Berlin-Göttingen-Heidelberg.
Urey, H. C.: 1967, *Quart. J. Roy. Astron. Soc.* **8**, 23.
Warner, B.: 1968, *Monthly Notices Roy. Astron. Soc.* **139**, 115.